A Spiking Neural Network-based Model for Anaerobic Digestion Process

G. Lo Sciuto[1], G. Susi[2], G. Cammarata[1], G. Capizzi[1]
[1]Department of Electrical, Electronics, and Informatics Engineering, University of Catania
Viale A. Doria 6-95125, Catania (Italy)
[2]Department of Electronics Engineering, University of Rome "Tor Vergata" Rome
Via Orazio Raimondo, 18 - 00173 Rome (Italy)

***Abstract*— There are many conversion technologies for the transformation of biomass into usable energy forms. Among these technologies, anaerobic digestion is one of the most attractive. In many papers appeared in the literature it has been demonstrated that the application of efficient mathematical models is an essential requirement to improve digester's performance. In this paper a spiking neural network-based model for anaerobic digestion process is proposed. This model performs a long-term prediction of the concentration of the biogas (CH_4 and CO_2) at the 100^{th} day of the process, by analysing the concentration evolution of 6 measurable marker-molecules (MMM) namely CH_4, CH_4S, CO_2, H_2, H_2S and NH_3 during the first 10 days of the process. For the validation of the model, a small domestic digester was realized. The tests carried out show an excellent agreement between the predicted values and those obtained with the digester.**

Keywords—Biogas; biogas prediction for food waste; anaerobic process models; spiking neural network

I. INTRODUCTION

The depletion of conventional fuels and the increasing global warming will force us to seek clean alternative energy resources [1-3]. Among various alternatives the biomasses have aroused a great interest as potential feedstock for clean energy production.

There are many conversion technologies for the transformation of biomass into usable energy forms. These can be classified as: direct combustion, pyrolysis, gasification, liquefaction, supercritic fluid extraction, anaerobic digestion, fermentation, acid hydrolysis, enzyme hydrolysis, and esterification. Among the above-mentioned technologies, anaerobic digestion is one of the most attractive. The attractiveness is due to the various beneficial properties of the process:

- Good waste management.
- Anaerobic digestion is not only feasible in large-scale industrial installations, but can also be applied on a small scale.
- Improved fertilization efficiency.
- Less nuisance from odors and flies.
- Less greenhouse gas emission.

Anaerobic digesters convert organic waste (agricultural and food waste, animal or human manure, and other organic waste), into biogas.

Biogas is a mixture of CH4, CO2, a small amount of nitrogen, water vapor and other gases. CH4 is the simplest hydrocarbon that can be used as a biofuel to produce energy.

In many papers appeared in the literature it has been demonstrated (for a review see [4]) that the application of efficient mathematical models is an essential requirement to improve digester's performance.

Several mathematical models that have been proposed, describe the anaerobic digestion process [5-9], but each of these models describes only some aspects of the anaerobic digestion process.

One of the few models capable of predicting with a certain approximation the major processes occurring in an anaerobic digestion system is ADM1 [10], but this model (as the other) is not able to predict the exact methane concentration evolution over the time of the process.

In this paper a spiking neural network-based model for anaerobic digestion process is proposed. This model performs a long-term prediction of the concentration of the biogas (CH_4 and CO_2) at the 100^{th} day of the process, by analysing the concentration evolution of 6 measurable marker-molecules (MMM) namely CH_4, CH_4S, CO_2, H_2, H_2S and NH_3 during the first 10 days of the process. The model is based on two SNN-based subsystems, one for CH4 and one for CO_2, that are globally trained in a supervised manner, using the 10 days time-series of the marker molecules concentrations (i.e.: early-stage evolutions) as input, and the 100^{th} day biogas concentration value (long term values) as target. This represents a prediction on the quantity of energy available from the digestion process.

The data used to train the neural network have been obtained by means of extensive simulations carried out with the COMSOL Reaction Engineering Lab commercial software. While for the validation of the model, a small domestic digester was realized.

Test results show an excellent agreement between the predicted values and those obtained with the digester.

To the best of our knowledge this is the first spiking neural

network-based model for anaerobic digestion process.

II. Biochemical Process of Anaerobic Digestion

Anaerobic digestion is a degradation process of biodegradable waste in the absence of oxygen. The whole process is composed of four main stages, carried out by different microbial communities [11]. The four major stages of the anaerobic digestion are: Hydrolysis, Acidogenesis (acidification phase), Acetogenesis and Methanogenesis. The anaerobic digestion process proceeds efficiently if the degradation rates of all three stages are equal.

In fig. 1 is shown a schematic representation of the anaerobic digestion process.

A. Hydrolysis

In the stage of the hydrolysis of polymerized mostly-insoluble organic compounds, like carbohydrates and proteins, fats are decomposed into soluble monomers and dimers, that is, monosaccharides, amino acids, and fatty acids. Hydrolysis of hardly decomposable polymers, that is, cellulose and cellulocottons is considered to be a stage which limits the rate of wastes digestion. The rate of hydrolysis process depends on parameters such as size of particles, pH, production of enzymes, diffusion, and adsorption of enzymes on the particles of wastes subjected to the digestion process. For many enzymes, the rate of catalysis varies with the concentration and thickness of the substrate.

Generally the rate of the chemical reactions involved in the hydrolysis process rises with the temperature. In the experiments carried out in this work we have used the Arrhenius equation in order to relate the rate of chemical reactions with the temperature.

The Arrhenius equation is defined as:

$$k = A \cdot e^{\frac{-E_a}{R*T}} \tag{1}$$

where k is the rate coefficient, A is a constant, E_a is the activation energy, R is the universal gas constant, and T is the temperature (Kelvin). The values of the constants A and E_a depend on the composition, concentration and thickness of the substrates

B. Acidogenesis

During this stage, the acidifying bacteria convert water-soluble chemical substances, including hydrolysis products, to short-chain organic acids (formic, acetic, propionic, butyric, and pentanoic), alcohols (methanol, ethanol), aldehydes, carbon dioxide, and hydrogen. From protein decomposition we obtain amino acids and peptides which may be a source of energy for anaerobic microorganisms. For example, long chain fatty acids (LFCA) are degraded into volatile fatty acids (VFA) and hydrogen via oxidation.

In order to describe the biological kinetics of the chemical processes occurring in this phase, the Monod model [12] is commonly used . It describes microbial growth and substrate degradations in such applications as batch and continuous

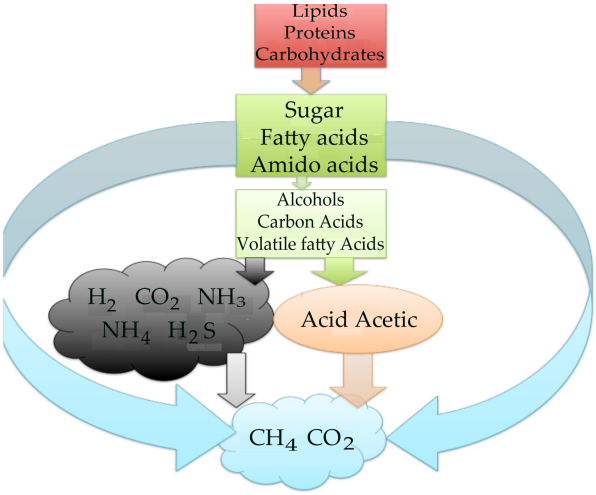

Fig. 1. The Anaerobic digestion process

fermentation, activated sludge waste water treatment. Much of its versatility is due to the fact that it can describe the biodegradation rates using a first-order kinetics with respect to the target substrate concentration. The model is determined by the first-order differential equation:

$$\eta'(t) = \mu(t) \cdot \eta(t) \tag{2}$$

where

$$\mu(t) = \mu_{Max} \frac{S(t)}{S(t) + K_s}$$

The parameter μ_{max} denotes the maximum growth rate, K_s is the saturation of affinity constant and $\eta(t)$ and $s(t)$ denote the concentration of micro-organisms and the concentration of the substrate respectively. The variable t represents the time, which varies in a compact interval [0, T]. The minimum value of T is several hours for optimal microbiological media, whereas the maximum is 1 year or more for specialized groups of microorganisms.

C. Acetogenesis

In this stage, different microbes and acetogenic bacterias convert the acid phase products into acetates and hydrogen which may be used by methanogenic. The ammonia and carbon dioxide created in previous stages are consumed. The main acids produced are acetic acid (CH_3COOH), propionic acid (CH_3CH_2COOH), butyric acid ($CH_3CH_2CH_2COOH$), and ethanol (C_2H_5OH).

D. Methanogenesis

This phase consists in the production of methane by meth-

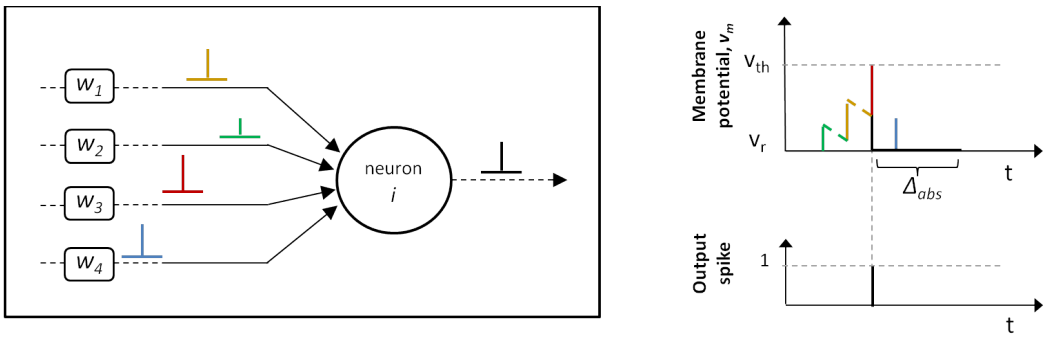

Fig. 2. Schematic representation of LIF neuron model operation. Input postsynaptic spikes are integrated until the threshold is reached. After, an output spike is immediately generated. Note that the more the input spikes are synchronized, the more the contributes are effective for the overcome of v_{th}. After, the membrane potential is instantaneously reset to to v_r and remains inactive for a period Δ_{abs} (that is why the fourth contribution has not been integrated by neuron i)

anogenic bacteria. Methane in this phase of the process is produced from substrates which are the products of previous phases, that is, acetic acid, H_2, CO_2, formate and methanol, methylamine or dimethyl sulfide.

III. A Brief Overview on Spiking Neural Networks

The Spiking neural networks (SNNs) are similar to the traditional neural networks [13-14] but they also incorporate the concept of time into their neurons and synaptic weights.

Therefore, in a synthetic way, we can say that the SNNs are networks of spiking neurons.

A spiking neural network is basically composed of a number of spiking neurons (i.e., basic elements able to emit pulses), some of which are connected by synapses. Each couple of connected neurons $j \rightarrow i$ is characterized by its *synaptic weights* (i.e., w_{ij}). The spatial information can be encoded in SNN as locations of synapses and neurons, while the temporal information (time) on the spiking activity of the SNN [15].

The behavior of a real neuron is very complex and most widely used models of spiking neurons can be expressed in the form of ordinary differential equations. For this reason the choice of a spiking neuron model is usually a trade-off between biological plausibility and complexity [16].

Among the models of spiking neurons present in literature, Leaky Integrate-and-Fire (LIF) model is very fast to simulate, and particularly attractive for large-scale network simulations. This model is characterized by two peculiarities:

1. The neuron is modeled as a "leaky integrator" of its inputs: if no input event occurs, the membrane potential (v_m, that is the internal state of a neuron) slowly decreases to zero with a proper behaviour (i.e.: *under-threshold decay*).
2. When the membrane potential reaches the *firing threshold* v_{th} , it is instantaneously reset to the *resting potential* v_r , and the neuron fires a spike.

In some spiking network tools, the under threshold decay behavior is approximated as linear, and LIF can be simply defined by three parameters:

- Linear leak rate (l).
- Firing threshold (v_{th}).
- Refractory period (Δ_{abs}).

In this case, starting from an initial value $v_{m,i}$, the membrane potential of neuron i will increase of the quantity w_{ij} every time that a spike arrives from neuron j:

$$v_{m,i}(t) = v_{m,i}(t-1) + w_{i,j} \tag{3}$$

Between spikes, the membrane potential leaks according to the leak rate:

$$v_{m,i}(t) = v_{m,i}(t-1) - l \tag{4}$$

If $v_{m,i}$ overcomes the threshold, a spike is generated in output:

$$s_i(t) = \begin{cases} 1 & if \quad v_{m,i}(t-1) \geq v_{th} \\ 0 & otherwise \end{cases} \tag{5}$$

and it is received by all the subsequently connected neurons. In case of spike generation, the membrane potential will keep to zero for an interval equal to Δ_{abs}.

Neurons in the network are connected by links (i.e.: synapses) characterized by synaptic weights which permit to modify the amplitude of the passing pulses. Synapses can vary according to the activity of the network by means of synaptic plasticity.

In Fig. 2 is shown a schematic representation of the LIF neuron model operation.

A. Synaptic Plasticity: Spike Timing Dependent Plasticity

Synaptic plasticity is the ability of synapses to strengthen or weaken over time, in response to increases or decreases in their activity. A well-known type of synaptic plasticity is defined by the precise timings of pre-pulse and post-pulse referred to neuron i influencing the magnitude and direction of change of the synaptic strength. This rule is known as the *spike-timing-*

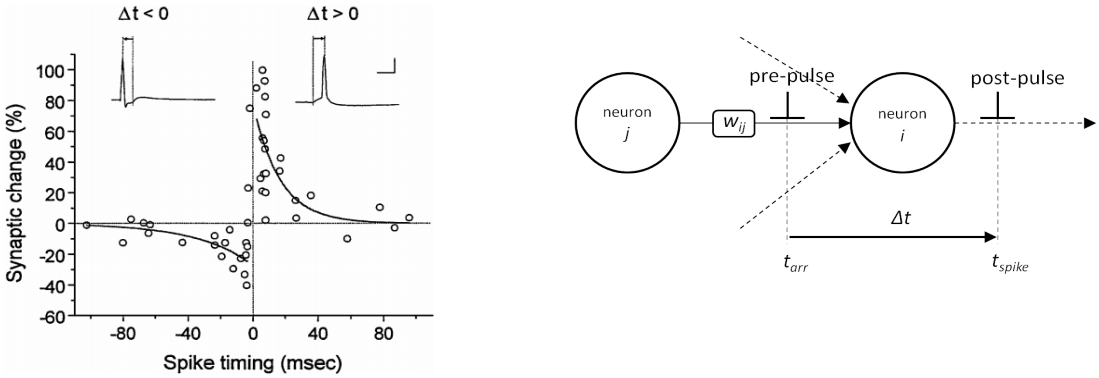

Fig. 3. STDP behaviour. On the left is represented the original curve extracted from Bi and Poo through experimental setup. The variation of synaptic weight is plotted as a function of the relative timing between presynaptic spike arrival and postsynaptic firing. The right curve represents the change of the synaptic weight when a pre-pulse arrives to the neuron i before the post-pulse is generated; the left curve represents the change of the synaptic weight when a post-pulse is generated from neuron i before the pre-pulse arrives. On the rigth Δt is represented, referred to the synapse w_{ij}. Note that $\Delta t = t_{spike} - t_{arr}$

plasticity (STDP) discovered by Bi and Poo through an experimental protocol [17], [18]. The STDP behavior can be approximated by two exponential functions, as shown in Fig 3.

For a pre-pulse at arrival time t_{arr} and a post-pulse at arrival time t_{spike}, the relative modification in synaptic strength $\Delta w_{ij}/w_{ij}$ is given by:

$$\frac{\Delta w_{ij}}{w_{ij}} = \begin{cases} A_{-} e^{\left(\frac{\Delta t}{\tau^{-}}\right)} & if \quad \Delta t < 0 \\ 0 & if \quad \Delta t = 0 \\ A_{+}\, e^{\left(-\frac{\Delta t}{\tau^{+}}\right)} & if \quad \Delta t > 0 \end{cases} \qquad (6)$$

where the parameters A_+, A_-, τ^+, τ^- are obtained during the training phase.

Many variants of this algorithm are used in order to capture space-time relationships from the encoded data [19].

IV. The Proposed SSN Based Model for Anaerobic Digestion Process

The proposed model consists of the long-term prediction of biogas production, starting on the sensing of concentrations of some gases during the early-stage of the process. Indeed the whole process of methane production by anaerobic digestion depends on the chemical processes occurring during the early stage of the process: the effects of parameter variations in the first days have a strong influence on process evolutions (Hydrolysis, Acidogenesis, etc.), and consequent slowing/ speeding-up of biogas production.

In this paper it was carried out the long-term prediction of the concentration of the biogas (CH4 and CO2) at the 100th day of the process, analysing the concentration evolution of the 6 MMM. The model is based on two SNN-based subsystems, one for CH4 and one for CO2, that are globally trained in a supervised manner, using the 10 days time-series of the marker molecule concentrations (i.e.: early-stage evolutions) as input, and the 100th day biogas concentration value (long term values) as target. This represents a prediction on the quantity of energy

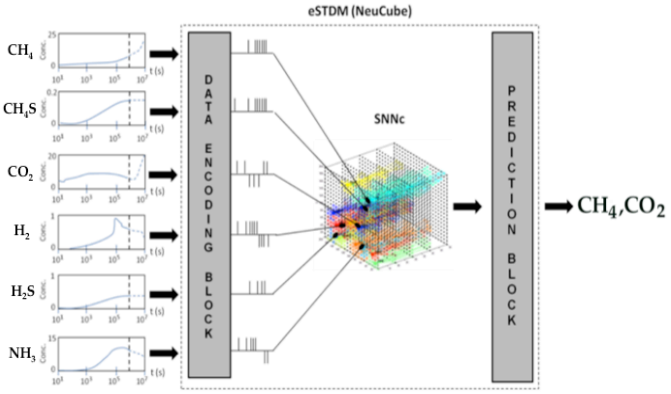

Fig. 4. The the predictive structure is composed of three main modules: data encoding block, SNN block, prediction block.

available from the digestion process. In order to train this neural network, we have used the concentration values of simple gases obtained by Comsol simulations.

For the implementation of the predictive structure, we have used the *NeuCube* computational framework [20]. The structure consists of three different blocks: data encoding block, SNN block and prediction block (see Fig. 4), that will be described as follows.

A. Data Encoding Block

This block is able to encode the information carried out by the time series of the MMM concentrations in the form of spike sequences.

Each one of the 6 MMM concentration evolutions has been described (sub-sampling the 6 MMM time series) by a *100-samples vector*, representing the first 10 days of the process (early stage period).

The data vector has been transformed into a spike train applying the thresholding representation (TR) algorithm [21] to the 100-samples vector, with a threshold of 0.2. It allows to generate spike sequences composed of both excitatory and in-

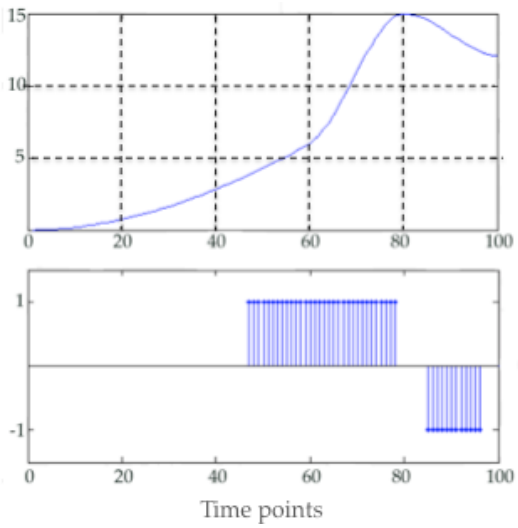

Fig. 5. The NH_3 data Encoding (*100-samples vector*) into trains of spike using TR algorithm. Top: concentration's evolution of NH_3 during the first 10 days of anaerobic digestion process. Bottom: corresponding spike train obtained applying TR algoritm.

hibitory contributes, corresponding respectively to an increase or a reduction in signal amplitude without the need of normalization preprocessing steps such as scaling, smoothing, etc.. An example of encoding data into trains of spikes using TR algorithm is shown in Fig. 5.

B. *SSN block*

In the second block spike trains were presented to the interconnected LIF neurons (the neuron of the neural network), the SNN cube (SNNc).

The SNNc is trained in an unsupervised mode, where the initial set of connection weights is modified to encode hidden spatio-temporal relationships from the input data into neuronal connection weights. Polychronization effect [22] makes the SNNc able to activate the same groups of spiking neurons with a similar spike-timing pattern when a similar input is presented. Progressively, the spike timing dependent plasticity (STDP) mechanism modulates the connection weight between two neurons, in relation to their temporal order of activation [22]. Since the used variables don't have spatial information, these have been mapped taking into account the temporal similarity between them, as proposed in [23]. Variables with increased temporal similarity have been mapped in spatially closer input neurons of the SNNc. In order to estimate the temporal similarity between time series, we have computed the Pearson correlation coefficient [23] for any couple of input vectors. Then we used this correlation coefficient to measure the distance between the input neurons (NeuCube features). The proximity between two neurons then is established using the following formula:

$$D_n = \lfloor D_{max} \cdot (1 - |p|) + 1 \rfloor \quad and \quad (0 < |p| < 1) \qquad (7)$$

where D_{max} is the maximum distance allowed between neurons (set by the user), p is the Pearson correlation coefficient and D_n is the mapping distance (expressed in terms of number of neurons). This procedure is able to infer to the SNNc regions an improved *anatomical connectivity* on the basis of the revealed *functional connectivity* [23].

Fig. 6. The anaerobic digester system.

Fig. 7. The fermentation vessel.

C. *Prediction block*

The second learning stage occurs in the SNN block: the spiking neurons of this block are trained to associate the spiking patterns generated by the SNNc to the target values.

The Prediction block is an output neural structure trained *functional* via supervised learning method, using the dynamic evolving SNN (deSNN) algorithm [24], that makes use of both rank-order (RO) [25] and spike driven synaptic plasticity (SDSP) learning rules [26]. RO learning will set the initial values of weights and SDSP rule adjusting them based on further incoming spikes.

The proposed method implies that this block operates as a regressor: the same data used for the train of SNNc are used also to train the prediction block in order to associate input data $\underline{\mathbf{x}}$ to target $\mathbf{y}$.

V. The Anaerobic Digester: Experimental Setup

The realized digester consists of a stainless steel reactor (see Fig. 6) with the inside surface sealed by a thin glass-fiber layer reinforced to overcome the problem of corrosion and to make it gas-tight.

The fermenter vessel has a capacity of approximately 24 litres and an operating pressures of 0 Barg (see Fig. 6). The oth-

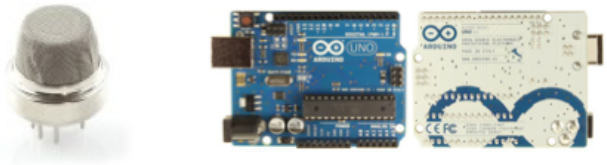

Fig. 8. The MQ-4 gas sensor (left) and Arduino Board (rigth).

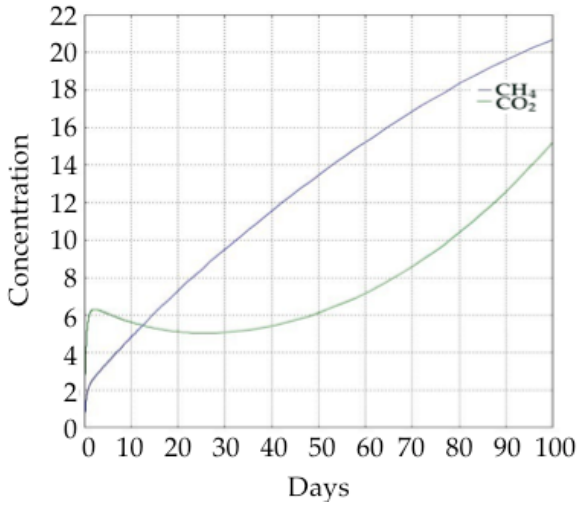

Fig. 9. The biogas composition over the time.

ers components of the biodigester are: transparent tubular polyethylene, gas exit PCV pipe, inlet PCV pipe. The inlet pipe has a valve to allow the emptying of the reactor. For the conveying gas, to the coupling flange of the expansion vessel, it has been used a brass fitting.

In the biodigester a water filter (15 cm) is used as a hydraulic guard and a second filter, with caustic soda and active carbon, is used to remove the carbon dioxide and the hydrogen sulfide. The compressor is connected to the valve preload of the expansion vessel, in order to compress the gas and store it in another tank, thus eliminating the contact between air and gas, particularly dangerous for the formation of explosive mixtures of air and gas.

To obtain an uniform mix of food waste and vegetable waste within the reactor we used an electrical agitator with added water in order to facilitate the growth of thermophilic microbes for faster degradation of waste.

The gas detection system consist of an MQ-4 gas sensor and an Arduino Board that is connected to the output voltage of the gas sensor. The MQ-4 gas sensor and Arduino Board are shown in Fig. 8.

The MQ-4 gas sensor detects natural gas concentrations composed of mostly Methane CH_4 from 200 to 10000 *ppm*. This sensor has a high sensitivity to Methane and fast response time. When the gas sensor MQ-4 detects the presence of gas, it sends an analogue signal to the AD-converter of the Arduino board.

It has been observed the operation of the biogas system for

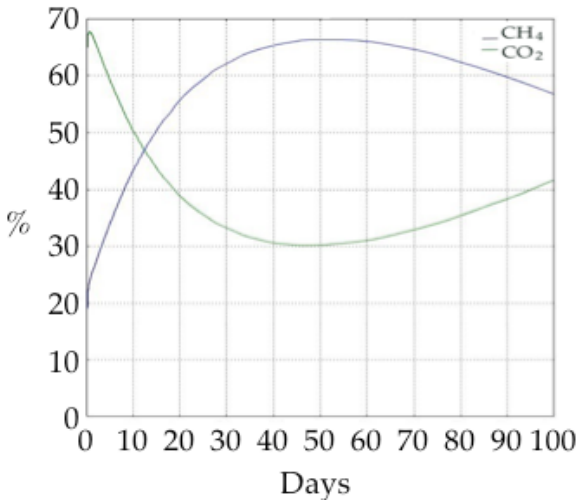

Fig. 10. The relative biogas composition over the time.

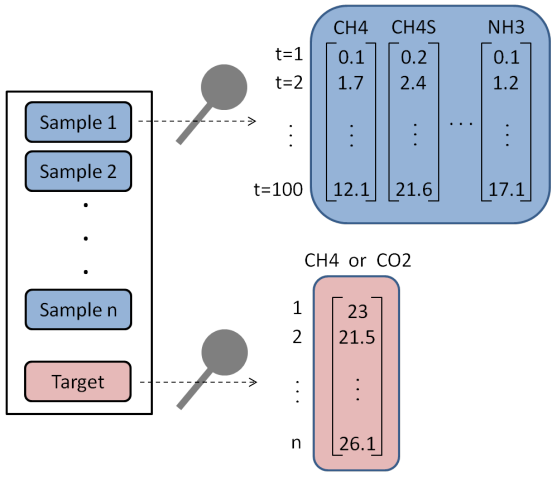

Fig. 11. The structure of the datasets

100 days, storing gas pressure and concentration data starting from few hours after the first loading of the biomass in the digester.

VI. Training Data for SNNs Obtained By Comsol Symulations

In order to form a statistically significant train pattern, used to train the SNN, we simulated 50 reactions including hydrolysis, acidogenesis, acetogenesis and methanogenesis by means of the "COMSOL Reaction Engineering Lab" software, that automatically solves material and energy balances including the complicated reaction-rate expressions of dry anaerobic digestion of food waste, which was investigated under mesophilic conditions, in a Batch reactor with a temperature of 32°C. The simulation time was set equal to 100 days.

The values of the activation energy E_a and of the constant A of the equation (1), used for the substances involved in the hydrolysis process are reported in Tables I and II.

Four different kinds of substrate concentrations have been

analyzed for the biogas process: Carbohydrates, Proteins, Lipids and Water. We carried out a lot of simulations of the anaerobic digestion process by changing the substrate compositions. In all simulations the water was used as a solvent.

In Fig. 9 (concentrations in mol/m^3) and Fig. 10 (relative concentrations) we can observe the change in percentage of the biogas composition. These graphs were obtained by using, in the simulation, the concentrations of carbohydrates, proteins and lipids shown in Table III.

Initially, the biogas consists of almost 70% carbon dioxide and 30% methane. After ten days, the production of methane exceeds that of carbon dioxide up to a maximum limit of about 66%. While after about 50 days, there is again a reversal and the production of methane drops considerably.

VII. Simulation Results

Two different datasets have been generated from Comsol simulations: one for the prediction of CH_4, and the other for CO_2. From each simulation it has been generated one training data structure (sample). This structure is constituted by a 100 x 6 matrix composed by the 6 time series of the MMMs (early-stage evolutions), obtained by one Comsol simulation. The target is represented by the concentration values of the biogas after 100 days (long-term values). The structure of the datasets is shown in Fig. 11.

For both of the two SNN-based subsystems, the SNNc is composed of 125 neurons ($X = 5$, $Y = 5$, $Z = 5$), connected in a "small world" topology with a radius of 2. The 6 input neurons have been positioned according to the relative signal temporal similarity, as described in subsection "SNN block".

The dataset has been divided into three groups: training set (50%), model selection or validation set (25%) and recall or test set (25%).

In order to develop the optimum network model, many networks have been trained. The optimisation of the parameters of NeuCube has been achieved by trial and error tests on the SNN models. The optimal values of the parameters for the two SNNc (one for CH_4, one for CO_2) are:

$CH_4 - SNNc$	$CO_2 - SNNc$
$STDP\ rate\ =\ 0.02$	$STDP\ rate\ =\ 0.01$
$Threshold\ of\ firing\ =\ 0.5$	$Threshold\ of\ firing\ =\ 0.5$
$Potential\ leak\ rate\ =\ 0.002$	$Potential\ leak\ rate\ =\ 0.002$
$Refractory\ time\ =\ 8$	$Refractory\ time\ =\ 6$

The optimal values of the parameters *mod, drift, k and* σ for the two SNNc are respectively 0.8, 0.005, 3, 1 (for both the SNNc the parameters are the same).

The performance evaluations of the proposed model was made by using the data obtained by the digester.

The prediction errors have been calculated by means of the Mean Absolute Deviation (MAD), the Mean Absolute Percent Error (MAPE), and the Mean-Root-Squared Error (MRSE) [27]. The Mean Absolute Deviation (MAD), the Mean Absolute Percent Error (MAPE), and the Mean-Root-Squared Error (MRSE) are described as follows:

$$MAD = \frac{\sum_{i=1}^{n} |y_i - \hat{y}_i|}{n_t}$$

$$MAPE = \frac{\sum_{i=1}^{n} \left| \frac{y_i - \hat{y}_i}{y_i} \right|}{n_t} \cdot 100\ \%$$

$$MRSE = \frac{\sqrt{\sum_{i=1}^{n} (y_i - \hat{y}_i)^2}}{n_t}$$

where y_i is the experimental value, while $\hat{y}_i$ is the predicted value, and n_t is the total number of samples in the test set.

The obtained values of MAD, MAPE and MRSE for CH_4 are respectively: 0.962, 4.07, 0.47, while for CO_2 are: 1.958, 10.48, 0.923.

TABLE I. The Activation Energy E_A and The Constant A in the Hydrolysis of Cellulose

Substrate	**Starch**	**Cellulose**	**Cellobiose**	**Xylan**	**Xylose**	**Lactose**
A [s^{-1}]	2.9e06	6.6e14	5.1e04	7.8e13	2.4e14	6.19e08
Ea [kJ/mol]	4.17e04	1.1e05	3.9e04	1.1e05	1.1e05	4.27e04

TABLE II. The Activation Energy E_A and The Constant A in the Hydrolysis of Proteins

Substrate	**Milk Whey**	**Casein**	**Keratin**	**Collagen**	**Wheat**
A [s^{-1}]	2.11e07	1.9e07	1.9e04	3.25e17	17e14
Ea [kJ/mol]	6.3e04	2.93e04	2.03e04	1.03e05	3.43e04

TABLE III. The Concentrations of Carbohydrates, Proteins and Lipids (mol/m^3)

Carbohydrates	**Lipids**	**Proteins**
aC6H10O5=1	C57H104O6=0.6	KER=1
bC6H10O5=0.02	C51H98O6=1	GRA=2
cC5H8O4=0.01	C37H70O5=0.6	CAS=4
C12H22O12=20	C37H68O5=0.4	LGL=2
		LAL=1
		BSA=2
		COL=2

VIII. Conclusions

In this paper a spiking neural network-based model for anaerobic digestion process is proposed. This model performs a long-term prediction of the concentration of the biogas (CH4 and CO2) at the 100th day of the process, by analysing the concentration evolution of 6 measurable marker-molecules (MMM) namely CH4, CH4S, CO2, H2, H2S and NH3 during the first 10 days of the process.

The tests carried out with experimental data show very low values of MAD, MAPE and MRSE. On the other hand, because the networks have been trained using data from simula-

tions and have been tested with experimental data, low values of MAD, MAPE and MRSE demonstrate that the model works very well and has a good generalization capability.

Therefore, the proposed model can be proficiently used to improve digester's performance.

REFERENCES

[1] F. Bonanno, G. Capizzi, S. Coco, C. Napoli, A. Laudani and G. Lo Sciuto, "Optimal thicknesses determination in a multilayer structure to improve the SPP efficiency for photovoltaic devices by an hybrid FEM — Cascade Neural Network based approach," International Symposium on Power Electronics, Electrical Drives, Automation and Motion (SPEEDAM), pp 355-362, 2014.

[2] F. Bonanno, G. Capizzi and G. Lo Sciuto, "A neuro wavelet-based approach for short-term load forecasting in integrated generation systems," International Conference on Clean Electrical Power (ICCEP), pp. 772-776, 2013.

[3] F. Bonanno, G. Capizzi, G. Lo Sciuto and C. Napoli, "Wavelet recurrent neural network with semi-parametric input data preprocessing for micro-wind power forecasting in integrated generation Systems," International Conference on Clean Electrical Power (ICCEP), pp. 602-609, 2015.

[4] M. C. Tomei, C. M., Braguglia, G. Cento, G. Mininni, "Modeling of Anaerobic digestion of sludge ," Critical Reviews in Environmental Science and Technology, vol. 39, no. 12, pp. 1003-1051, 2009.

[5] R. Chouari, D. Le Paslier, P. Daegelen, P. Ginestet, J. Weissenbach, A. Sghir, "Novel predominant archaeal and bacterial groups revealed by molecular analysis of an anaerobic sludge digester" Environmental Microbiology, vol. 7, no. 8, pp. 1104-1115, 2005.

[6] S. G. Shin, G. Han, J. Lim, C. Lee, S. Hwang, "A comprehensive microbial insight into two-stage anaerobic digestion of food waste-recycling wastewater" Water Research, vol. 44, no.17, pp. 4838-4849, 2010.

[7] D. G. Cirne, A. Lehtomäki, L. Björnsson, L. L. Blackall, "Hydrolysis and microbial community analyses in two-stage anaerobic digestion of energy crops," Journal of Applied Microbiology, vol 103, no. 3, pp. 516-527, 2007.

[8] Curry Nathan, and Pragasen Pillay. "Biogas prediction and design of a food waste to energy system for the urban environment," Renewable Energy, vol. 41, 200-209, 2012.

[9] T. Beltramo, C. Ranzan, J. Hinrichs, B. Hitzmann, "Artificial neural network prediction of the biogas flow rate optimised with an ant colony algorithm," Biosystems Engineering, vol. 143, pp. 68-78, 2016.

[10] D. J. Batstone, et al., "The IWA Anaerobic Digestion Model No 1 (ADM1)," Water Sci Technol., vol. 45, no. 10. pp. 65-73, 2002.

[11] Fayyaz Ali Shah, Qaisar Mahmood, Mohammad Maroof Shah, Arshid Pervez, and Saeed Ahmad Asad, "Microbial Ecology of Anaerobic Digesters: The Key Players of Anaerobiosis," The Scientific World Journal, vol. 2014, Article ID 183752, 21 pages, 2014.

[12] H. Dette, V. B. Melas, A. Pepelyshev, and N. Strigul, (2003), "Efficient design of experiments in the Monod model," Journal of the Royal Statistical Society: Series B (Statistical Methodology), vol. 65, pp. 725–742.

[13] S. Haykin, "Neural Networks and Learning Machines", Englewood Cliffs, NJ: Prentice-Hall, 2008.

[14] F. Bonanno, G. Capizzi, S. Coco, A. Laudani and G. L. Sciuto, "A coupled design optimization methodology for Li-ion batteries in electric vehicle applications based on FEM and neural networks International Symposium on Power Electronics, Electrical Drives, Automation and Motion (SPEEDAM), pp. 146-153, 2014.

[15] H. H. Amin, "Spiking Neural Networks: Learning, Applications, and Analysis, LAP LAMBERT Academic Publishing , 2011.

[16] E. M. Izhikevich, "Which model to use for cortical spiking neurons? ," IEEE transactions on neural networks, vol. 15, no. 5, pp. 1063-1070, 2004.

[17] D. B. Sinha, N. M. Ledbetter and D. L. Barbour, "Spike-timing computation properties of a feed-forward neural network," Frontiers in Computational Neuroscience, vol. 8, 2014.

[18] Bi GQ and Poo MM, "Synaptic modifications in cultured hippocampal neurons: dependence on spike timing, synaptic strength, and postsynaptic cell type," J Neurosci. , vol. 18, no. 24, pp. 10464-72, 1998.

[19] E. Capecci, N. Kasabov, G. Y. Wang, "Analysis of connectivity in NeuCube spiking neural network models trained on EEG data for the understanding of functional changes in the brain: A case study on opiate dependence treatment," Neural Networks, vol.68, pp. 62-77, 2015.

[20] Available: http:// www.kedri.aut.ac.nz/neucube/

[21] Nikola K. Kasabov, "NeuCube: A spiking neural network architecture for mapping, learning and understanding of spatio-temporal brain data," Neural Networks," vol. 52, pp. 62-76, 2014.

[22] E. M. Izhikevich, "Polychronization: Computation with Spikes," Neural Comput., vol. 18, no. 2, pp. 245-282, 2006.

[23] E. Tu, N. Kasabov, J. Yang, "Mapping Temporal Variables Into the NeuCube for Improved Pattern Recognition, Predictive Modeling, and Understanding of Stream Data," IEEE Transactions on Neural Networks and Learning Systems , vol.PP, no. 99, pp. 1-13, 2016.

[24] K. J. Friston, "Functional and effective connectivity: a review," Brain connectivity, vol.1, no.1, pp. 13-36, 2011.

[25] N. Kasabov, K. Dhoble, N. Nuntalid, G. Indiveri, "Dynamic evolving spiking neural networks for on-line spatio-and spectro-temporal pattern recognition," Neural Networks, vol. 41, pp. 188-201, 2013.

[26] S. Thorpe, J. Gautrais, "Rank order coding," Computational Neuroscience, pp. 113-118, Springer US, 1998.

[27] G. Capizzi, F. Bonanno and C. Napoli, "Hybrid neural networks architectures for SOC and voltage prediction of new generation batteries storage," International Conference on Clean Electrical Power (ICCEP), pp. 341-344, 2011.